HHS Public Access

Author manuscript

Toxicol Pathol. Author manuscript; available in PMC 2021 January 15.

Published in final edited form as:

Toxicol Pathol. 2020 October ; 48(7): 887–898. doi:10.1177/0192623320961017.

Ozone reacts with carbon black to produce a fulvic acid-like substance and increase an inflammatory effect

Andrew J. Ghio[1], **David H. Gonzalez**[2], **Suzanne E. Paulson**[2], **Joleen M. Soukup**[1], **Lisa A. Dailey**[1], **Michael C. Madden**[1], **Beth Mahler**[3], **Susan A. Elmore**[4], **Mette C. Schladweiler**[1], **Urmila P. Kodavanti**[1]

[1]US Environmental Protection Agency, Research Triangle Park, North Carolina

[2]Atmospheric and Oceanic Sciences, University of California at Los Angeles, California

[3]Experimental Pathology Laboratories, Inc., Research Triangle Park, North Carolina

[4]National Toxicology Program, National Institute of Environmental Health Sciences, Research Triangle Park, North Carolina

Abstract

Exposure to ambient ozone has been associated with increased human mortality. Ozone exposure can introduce oxygen-containing functional groups in particulate matter effecting a greater capacity of the particle for metal complexation and inflammatory effect. We tested the postulate that 1) a fulvic acid-like substance can be produced through a reaction of a carbonaceous particle with high concentrations of ozone and 2) such a fulvic acid-like substance included in the PM can initiate inflammatory effects following exposure of respiratory epithelial (BEAS-2B) cells and an animal model (male Wistar Kyoto rats). Carbon black (CB) was exposed for 72 hours to either filtered air (CB-Air) or approximately 100 ppm ozone (CB-O_3). CB exposure to high levels of ozone produced water-soluble, fluorescent organic material. Iron import by BEAS-2B cells at 4 and 24 hr was not induced by incubations with CB-Air but was increased following co-exposures of CB-O_3 with ferric ammonium citrate. In contrast to CB-Air, exposure of BEAS-2B cells and rats to CB-O_3 for 24 hr increased expression of pro-inflammatory cytokines and lung injury respectively. It is concluded that inflammatory effects of carbonaceous particles on cells can potentially result from 1) an inclusion of a fulvic acid-like substance after reaction with ozone and 2) changes in iron homeostasis following such exposure.

Keywords

Ozone; fulvic acid; air pollution; iron; lung diseases; carbon black; fulvic acid-like substance; inflammation; rats

Corresponding Author: Andrew J. Ghio, Human Studies Facility, 104 Mason Farm Road, Chapel Hill, NC 27514, ghio.andy@epa.gov.

Declaration of conflicting interest statement

The authors declare no potential conflicts of interest with respect to the research, authorship, and/or publication of this article.

Disclosure

This report has been reviewed by the National Health and Environmental Effects Research Laboratory, United States Environmental Protection Agency and approved for publication. Approval does not signify that the contents necessarily reflect the views and policies of the Agency nor does mention of trade names or commercial products constitute endorsement or recommendation for use.

Introduction

The human lung is regularly exposed to a wide variety of particles with a respirable diameter (<10 μm). A shared clinical, physiological, and pathological presentation associated with exposure to disparate particles supports a common mechanism in the lung. Accordingly, a single pathway has been proposed through which the effects of all particles are generated.[1,2]

Inorganic particles including oxides and oxide minerals have oxygen-containing functional groups at their surface such as silanols (-Si-OH) in silica and silicate particles. The inhalation of particles with such surfaces comprised of oxygen-containing functional groups introduces an electronegative interface following their deprotonation at physiologic pH values. Among the cellular cations available for complexation by the particle surface, iron is kinetically favored as a result of its electropositivity, high affinity for oxygen-containing functional groups, and relative abundance. Following endocytosis of an inorganic particle, surface functional groups react with intracellular iron producing a coordination complex that results in a functional deficiency of the metal within the cell.[1] Comparable to exposure to a metal chelator, the response to the functional metal deficiency associated with particle exposure can include oxidative stress, cell signaling, transcription factor activation, and release of pro-inflammatory mediators prior to apoptosis [3–11]. This can eventually culminate in the development of tissue inflammation and fibrosis [1,12]. Exposure to other compounds and agents with an equivalent capacity to complex metal cations induces a comparable inflammatory and fibrotic injury in humans [13–15].

The complexation of cell iron is also relevant to particulate matter (PM) containing organic compounds (e.g. ambient and emission air pollution particles). Surface functional groups in this PM can include alcohol, diol, epoxide, ether, aldehyde, ketone, carboxylate, ester, phenol, and catechol groups. Following exposure, organic particles also complex metal available in cells and tissues via these surface functional groups.[2]

Humic substances (HS) are heterogeneous, amorphous, organic materials found in all terrestrial and aqueous environments. Three different fractions of HS exist: humic acid, fulvic acid, and humin. Humin is the fraction of HS that is insoluble in water at any pH value. The humic acid fraction is insoluble in water under acidic conditions (pH<2) but soluble at higher pH values. Fulvic acid is that fraction of HS soluble in water under all pH conditions and remains in solution after removal of humic acid by acidification. Tropospheric aerosols are suspensions of small solid and/or liquid particles in air that have negligible terminal fall speeds. A substantial mass fraction (up to 90%) of tropospheric aerosols is comprised of natural organic matter which chemically resembles HS with a mixture of aromatic, phenolic, and acidic functional groups, and was therefore designated “humic-like substances” (HULIS) [16–18]. This material shares chemical characteristics with HS but differs in having a smaller molecular weight and lower aromaticity; it more closely approaches fulvic than humic acid [18]. In one study, about 3% of ambient air particulate matter (PM) was estimated to be HULIS [19]. Combustion products including wood smoke and diesel exhaust particles (i.e. emission air pollution sources) similarly included HULIS which approximated 8% and 5% respectively[19–21]. As a result of having a variety of oxygen-containing functional groups (e.g. carboxylic and phenolic groups), HULIS

complexes metal cations [22–25]. The high content of oxygen-containing functional groups in HULIS favors the formation of complexes with numerous metals but the absolute value of the stability complex with iron is the greatest [26].

Comparable to air pollution particles, exposure to ambient ozone has been associated with increased lung inflammation and human mortality (including non-accidental and cardiovascular mortality) [27–30]. Ozonation of carbonaceous PM significantly enhances the inflammatory response to the particle.[31] The mechanism for the enhanced inflammatory effect is postulated to be an alteration of particle chemistry by ozone from a nontoxic to a toxic form. Such interaction between carbonaceous particles and ozone is supported by epidemiological, controlled exposure, animal, and *in vitro* investigation.[32–35] The interaction between ozone and PM is proposed to result in a particle with a greater capacity to induce iron sequestration resulting in an increased disruption in metal homeostasis and subsequent inflammation and fibrosis. We tested the postulate that 1) a fulvic acid-like substance can be produced through a reaction of a carbonaceous material with high concentrations of ozone and 2) such a fulvic acid-like substance included in the PM has a capacity to participate in the inflammatory effects following exposure to ozone by disrupting cell iron homeostasis.

Methods

Materials.

All reagents were from Sigma Co. (St. Louis, MO) unless specified otherwise. Carbon black (CB) was from Columbian Chemicals Company (Marietta, GA; CAS Registry Number: 1333-86-4; mean particle size provided as 0.042 micron). For cell and animal studies, suspensions of CB in cell media and normal saline were sonicated (on ice) to disaggregate the particles. Immediately prior to exposure, the particle was dispersed using a vortex agitator. Suwannee River fulvic acid (II) (SRFA) was obtained from the International Humic Substances Society (IHSS; St. Paul, MN).

Reaction of carbon black with filtered air and ozone.

CB (200 mg) was placed between two 47 mm Teflon filters (Teflo, Pall Life Sciences, Port Washington, NY) within a filter holder (Savillex, Eden Prairie, MN). The particle was exposed to either 1) filtered air at 16 cubic cm/minute for 72 hr (CB-Air) or 2) approximately 100 ppm ozone in zero air (scrubbed of contaminants) at 16 cubic cm/minute for 72 hr (CB-O_3). During the reaction, flow was directed against gravity to establish a fluidized bed. The resultant particles were stored in a test tube at room temperature and used within four weeks of exposure.

Analysis of materials.

Fluorescence excitation-emission matrix (Lumina Spectrometer, Thermo Scientific) and attenuated total reflection-infrared (ATR-IR) spectra were obtained. Fluorescence excitation-emission matrix spectra covering λ_{ex} = 200-600 nm and λ_{em} = 220-620 nm in 5 nm intervals were obtained with a Thermo-Scientific Lumina Fluorometer. Fluorometer parameters included an excitation/emission slit size of 10 nm and an integration time of 10

ms. For ATR-IR scans, in order to minimize solvent interferences, all samples were evaporated to dryness. CB-Air, CB-O_3, and SRFA were analyzed as solids.

Cell culture.

BEAS-2B cells (an immortalized line of normal human bronchial epithelium) were obtained from the laboratory of Dr. Curtis Harris, maintained in serum-free growth medium (KGM, Clonetics, San Diego, CA) in T75 tissue culture flasks, and employed for *in vitro* investigations. Cells (passages 68-85) were grown to 90-100% confluence on uncoated plastic twelve-well plates in KGM which is essentially MCDB 153 medium supplemented with 5 ng/ml human epidermal growth factor, 5 mg/ml insulin, 0.5 mg/ml hydrocortisone, 0.15 mM calcium, bovine pituitary extract, 0.1 mM ethanolamine and 0.1 mM phosphoethanolamine. Cytotoxicity was assayed using release of lactic dehydrogenase.

Cell iron concentrations.

BEAS-2B cells were exposed to 100 μg/mL CB-Air, CB-O_3, and SRFA in media for 4 hr. After removal of the CB-Air, CB-O_3, and SRFA, the media was replaced and cells were exposed to ferric ammonium citrate (FAC), used because it is both buffered and physiologically relevant, for 4 hr incubation. After completion of the incubation, the media was removed and the cells were washed with HBSS and scraped into 1.0 mL 3 N HCl/10% trichloroacetic acid (TCA). After hydrolysis at 70° C for 24 hr with precipitation of heme in the 10% TCA, iron (non-heme) concentration in the supernatant was determined (λ=238.204 nm) using inductively coupled plasma optical emission spectroscopy (ICPOES; Model Optima 4300D, Perkin Elmer, Norwalk, CT).

Cell ferritin concentrations.

BEAS-2B cells were exposed to 100 μg/mL CB-Air, CB-O_3, and SRFA in media for 4 hr. FAC was added to a final concentration of 200 μM and the incubation continued for 24 hr. After the media was removed, cells were washed with HBSS, scraped into 1.0 mL HBSS, and disrupted using five passes through a gauge 25 needle. The concentrations of ferritin in the lysates were quantified using an immunoturbidimetric assay (Kamiya Biomedical Company, Seattle, WA).

Interleukin (IL)-8 and IL-6 release.

BEAS-2B cells were exposed to 100 μg/mL CB-Air, CB-O_3, and SRFA in media for 4 hr. FAC was added to a final concentration of 200 μM and the incubation continued for 24 hr. IL-8 and IL-6 concentrations in cell media were measured using a multiplex assay kit (MSD, Rockville, MD).

Animal exposures.

All procedures related to care and handling of animals were performed in accordance with regulations stipulated by the American Association for Accreditation of Laboratory Animal Care (AAALAC) and all experiments were approved by the Animal Care and Use Committee of the National Health and Environmental Effects Research Laboratory at the U.S. Environmental Protection Agency. Wistar Kyoto (WKY) rats were employed as a result

of frequent utilization as an animal model in the field of air pollution. Following anesthesia with isoflurane, 12-week-old male rats (Charles River Laboratories, Raleigh, NC) weighing 278 ± 26 g (mean ± standard deviation) were intratracheally instilled with 1000 μL saline/kg body weight saline, 2000 μg/kg body weight CB-Air in saline, or 2000 μg/kg body weight CB-O_3 in saline. After 24 hr, rats were euthanized (>200 mg/kg intraperitoneally; Fatal-Plus, Vortech Pharmaceuticals, Dearborn, MI). The trachea was cannulated and lavaged with calcium- and magnesium-free phosphate buffered saline at 37° C (28 mL/kg body weight/ 0.6). The lavage included three in-and-out washes with the same aliquot of buffer followed by transfer to ice. The left lung was filled with 10% formalin at total lung capacity and stored for pathology.

Total cell counts in the lavage fluid were quantified using a coulter counter and cell differentials were determined after preparation of a cytospin slide. After centrifugation of the lavage fluid (600 g × 10 min), biochemical assays included albumin, total protein, LDH, and gamma-glutamyl transferase (GGT) (KONELAB, Thermo Electron Oy, Finland).

Following fixation, lung tissues were processed for paraffin embedding. Serial 6-μm sections through the lung tissues were placed on charged slides (A. Daigger & Co, Vernon Hills, Illinois) and routinely stained with 1) hematoxylin and eosin and 2) Perls' Prussian blue for histopathology review. Digital images were captured from slides scanned on the Aperio Scan Scope AT2 instrument (Aperio; Leica Biosystems Inc, Buffalo Grove, Illinois) using ImageScope software, version 12.3 (Aperio). Formatting of images for publication was completed using Adobe Photoshop CC version 19.1.0 (Adobe Systems Inc, San Jose, CA).

Statistics.

Data are expressed as mean values ± standard deviation (SD) unless specified otherwise. The minimum number of replicates for all measurements was six unless specified otherwise. Differences between multiple groups were compared using one- and two-way analysis of variance. Two-tailed tests of significance were employed. Significance was assumed at $p<.05$.

Results

Fluorescence excitation-emission matrix spectra.

The fluorescence spectrum of CB-Air is demonstrated (Figure 1A). This is compared to fluorescence spectra of CB-O_3 (Figure 1B). Finally, a spectrum for SRFA is provided (Figure 1C). The scans show that exposure of CB to high levels of ozone produced fluorescent organic material. Furthermore, the spectra of the CB-O_3 and the SRFA share peaks indicating similarities of fluorophores between CB-O_3 and SRFA.

Attenuated total reflection-infrared spectra.

The attempts to obtain ATR-IR spectra on CB-Air were unsuccessful as a result of the small amount of organic material in samples. The ATR-IR spectra with the CB-O_3 were considered low quality but important features were noted. This can be compared to the ATR-IR spectrum with SRFA. Common infrared absorbances and functional groups between CB-

O_3 and SRFA are summarized (Table 1). The scans show that the exposure of CB to high levels of ozone produced an organic material which shares functional groups with fulvic acid including C=C and C-H from aromatic systems and C=O from carboxylic acids, ketones and aromatic systems. A difference between CB-O_3 and the SRFA samples is the absence of a strong alkane C-H peak in the CB-O_3 spectra.

Inflammatory effect of cell exposures.

In BEAS-2B cells, there was no significant cytotoxicity following 24 hr exposure to 100 μg/mL CB-Air, CB-O_3, and SRFA. Cell exposure to either CB-Air or CB-O_3 alone did not alter cell iron concentration, reflecting low concentrations of metal in the CB particles and the media (Figure 2A). BEAS-2B cell exposure to FAC for 4 hr resulted in an elevation in cell iron concentration, supporting increased iron import (Figure 2A). Iron import at 4 hr increased even further with inclusion of CB-O_3 and SRFA with FAC (Figure 2A). Twenty-four hr exposures to media, CB-Air, CB-O_3, and SRFA with and without FAC demonstrated the same pattern of metal uptake (Figure 2B). Iron concentrations in BEAS-2B cells did not change after exposures to media, CB-Air, CB-O_3, and SRFA but did not increase with inclusion of FAC. Those BEAS-2B cell exposures which included either CB-O_3 or SRFA along with FAC elevated cell metal to the greatest levels. The quantity of cell ferritin, an iron storage protein, was measured at 24 hr. The levels of ferritin were increased following exposure of BEAS-2B cells to FAC but those values following exposures of CB-O_3 and SRFA with FAC were greatest, mirroring import of iron at both 4 and 24 hr (Figure 2C). Inclusion of CB-O_3 with the FAC significantly elevated the ferritin level to values greater than concentrations of this storage protein following CB-Air and FAC, supporting an interaction between CB and ozone which mediated changes in cell iron homeostasis.

Release of pro-inflammatory mediators by respiratory epithelial cells exposed to media, CB-Air, CB-O_3, and SRFA with and without FAC was determined. Exposure of BEAS-2B cells to CB-Air for 24 hr did not increase the concentrations of either IL-8 or IL-6 in the supernatant relative to media (Figures 3A and 3B). However, exposure to CB-O_3 elevated the release of both pro-inflammatory mediators by the cells and this was comparable to exposure to SRFA (Figures 3A and 3B). Incubation of BEAS-2B cells with FAC alone had no significant effect on cytokine release at 24 hr (Figures 3A and 3B). Similarly, cell incubations with both CB-Air and FAC did not significantly change the concentrations of released IL-8 and IL-6 (Figures 3A and 3B). However, co-exposure of the BEAS-2B cells to FAC and either CB-O_3 or SRFA significantly decreased supernatant levels of the interleukins relative to exposures to CB-O_3 and SRFA alone (Figures 3A and 3B).

Inflammatory effect of animal exposures.

Relative to instillation of saline, rats exposed to CB-Air did demonstrate an elevation of a lavage biochemical endpoint (i.e. GGT) supporting lung injury (Figures 4A–4D). However, exposure of the rats to CB-O_3 at the equivalent dose significantly increased all lavage indices of inflammatory injury (i.e. albumin, total protein, LDH, and GTT) relative to CB-Air (Figures 4A–4D). Exposure to CB-Air elevated the lavage percentage of neutrophils but CB-O_3 increased both lavage neutrophils and eosinophils (Figures 4E and 4F).

Histopathologic evaluation of lung tissue revealed that all animals treated with CB-Air and CB-O_3 showed small, black, punctate particles scattered throughout the lung (Figures 5 and 6) which were either extracellular and free within the alveolar space or were intracellular within alveolar macrophages. Occasionally, large aggregates of particles were present in the terminal bronchi and alveolar ducts of animals in the CB-O_3 group (Figure 6C). In general, a greater number of particles and particle aggregates were noted in animals exposed to CB-O_3. Large, multifocal areas of macrophage infiltrates were present in areas with increased particles and macrophage aggregates were more frequent in those rats instilled with CB-O_3 (Figure 7A). Perivascular and peribronchial granulocytic infiltrates were present in the CB-Air but increased in the CB-O_3 groups (Figure 7B). There were no infiltrates in those animals instilled with saline. Bronchioalveolar lymphoid aggregates (BALT) were increased in the CB-O_3 relative to the CB-Air group (Figure 8B) and germinal centers were more prevalent and prominent (Figure 8C).

Discussion

CB is a paracrystalline carbon with few surface oxygen-containing functional groups; elemental analysis confirms oxygen content as usually 5% or less [36]. The product of the reaction between CB and ozone (CB-O_3) revealed fluorescence excitation-emission matrix spectra different from CB and resembling a reference fulvic acid. The ATR-IR scan of CB-O_3 also resembled fulvic acid with oxygen-containing functional groups. These data indicate that ozone has a capacity to change a carbonaceous material by introducing additional oxygen-containing functional groups, including carboxylates. After reacting with ozone, carbonaceous products have been demonstrated to have increased surface functionalization [37–41]. The resultant oxygenated groups were largely carboxylates, but other moieties (e.g. aldehyde and ketonic) can be observed. High-resolution X-ray photoelectron spectroscopy and Fourier transform-infrared spectroscopy previously confirmed that the surface oxygen introduced on the CB after reaction with ozone is most frequently present in carboxylic acid groups [42]. A smaller formation of phenols, lactones and quinones was noted after reaction of the CB with ozone[43]. Soot, a mixture of elemental carbon and organic compounds, can similarly be oxidized with a generation of polar surface groups including carboxylates [44] Such oxidation generates oxygen-containing functional groups, increasing the polarity of soot surfaces, thus increasing water-solubility [45–47] Oxidation of hexane soot formed carboxylates which were the only water-soluble organic compounds generated. It has also been demonstrated that fulvic acid can further react with ozone to generate aliphatic carboxyl and carbonyl compounds [48]. In the atmosphere, elevated ozone levels can be associated with increased concentrations of dicarboxylates [49].

In the respiratory tract, inorganic particles demonstrate a capacity to accumulate iron from available cell sources, reflecting the ability of surface functional groups to complex host metal [50,51]. After exposure, carbonaceous particles (e.g. coal, cigarette smoke and wood smoke particles) also complex metal available in cells and tissues via oxygen-containing, surface functional groups [12,19,52–54] Quantification of total acidity and carboxylates on these carbonaceous particles can demonstrate a presence of functional groups with a capacity to complex metals [22]. In this study, the reaction of the CB with O_3 yielded a product with increased numbers of oxygen-containing functional groups, including carboxylates,

predicting a greater capacity to complex iron and disrupt homeostasis of this metal. In support of this, exposure of respiratory epithelial cells to CB-O_3 increased cell iron concentrations and ferritin to higher levels, relative to CB-Air, after incubations with FAC. This is comparable to a reference fulvic acid recognized to have high concentrations of carboxylic, phenolic, and other oxygen-containing functional groups. Following exposure, this carbonaceous material will be endocytosed. With such intracellular transport, cell sources of iron can be complexed by the oxygen-containing functional groups included in the particle. The interaction between the particle and the cell will result in a deficiency of iron. Subsequently, metal is imported to meet the demands of the cell and the particle. A new equilibrium is attained with higher concentrations of cell iron. Some portion of this increased metal is stored in ferritin and cell levels of this storage protein also increase.

Comparable to other compounds with a capacity to sequester iron from the host cell, the response to the functional metal deficiency following CB-O_3 will include oxidative stress, cell signaling, transcription factor activation, and release of pro-inflammatory mediators[3–11]. This response can be observed following human exposure to PM which contains carbonaceous compounds[52,55]. The sequestration of iron, and an associated deficiency of cell metal after exposure to the standard fulvic acid, initiates pathways leading to injury and disease[53,56–62]. Accordingly, while CB-Air did not change the release of pro-inflammatory mediators, CB-O_3 significantly increased IL-6 and IL-8 levels. Exposure to other xenobiotic agents with an equivalent capacity to complex metal cations induces a comparable inflammatory response in humans[13–15]. Reflecting this increased capacity to initiate inflammation, animals exposed to CB-O_3 demonstrated a significantly greater inflammatory injury relative to those exposed to CB-Air. Lavage indices revealed more significant disparities than did inspection of the lung tissue itself.

Prior investigation has demonstrated that exposure to CB does not increase inflammatory endpoints and it is frequently employed as a control particle [63]. In a prior animal study, exposure to CB did not cause lung inflammation while ozone did [31]. However, exposure to both CB and ozone significantly enhanced the inflammatory response [31]. The mechanism for the enhanced inflammatory effect was postulated to be an alteration of the chemistry of the particulate by ozone from a nontoxic to a toxic form. Such interaction between particles and ozone is supported by epidemiological, controlled exposure, animal, and *in vitro* investigations [31–35,64] The results of this investigation suggest that a modification of CB by ozone (e.g. carboxylation to a HULIS) may participate in such an interaction with changes in lavage endpoints and increased 1) macrophage infiltrates, 2) perivascular and peribronchial granulocytic infiltrates, and 3) BALT present histologically in the CB-O_3 exposed animals relative to the CB-Air group exposed animals. Dissimilarities in particle number and diameter in the lungs of animals exposed to CB-Air and CB-O_3 may indicate differences in clearance although how a reaction of PM with ozone could change this endpoint is not obvious. In cultured cells, an interaction of ozone and CB has been demonstrated using electron microscopy methodology which results in a greater penetration and subsequent number of particles [65]. This was postulated to result from a damage of biological membranes by ozone allowing increased particle entry into biological systems. However, while not previously reported, the observation of a greater number and larger particles after animal exposure to CB-O_3, relative to CB-Air, may reflect an artifact of

intratracheal delivery. Treatment of the CB with ozone can possibly modify the hydrophobic character of the particle, allow its greater dispersion in aqueous buffer/medium, and result in a greater dose delivery to cells and animals. Interactions between ozone and CB must be further investigated using both cell and animal models.

It is concluded that inflammatory effects of carbonaceous particles on cells can result from 1) the inclusion of a fulvic acid-like substance following reaction of carbonaceous PM with ozone and 2) changes in iron homeostasis following such exposure. This observation of a production of a fulvic acid-like substance following the reaction between ozone and carbonaceous particles has a distinct significance. As a result of its water-solubility, fulvic acid-like substance in CB-O_3 is predicted to have some ability for transport into the blood with ensuing systemic distribution[18]. The capacity of these substances to initiate iron sequestration may change oxidative stress, signaling, transcription factor activation, release of pro-inflammatory mediators, apoptosis, inflammation, and fibrosis in extrapulmonary tissues. This supports potential associations of ozone exposure with extrapulmonary disease including coronary artery and cerebrovascular diseases [30].

Acknowledgments

Funding

The author(s) disclosed receipt of the following financial support for the research, authorship, and/or publication of this article: This work was supported [in part] by the NIH, National Institute of Environmental Health Sciences and the Environmental Protection Agency.

References

1. Ghio AJ, Tong H, Soukup JM, et al. Sequestration of mitochondrial iron by silica particle initiates a biological effect. Am J Physiol Lung Cell Mol Physiol. 2013;305(10):L712–724. [PubMed: 23997175]
2. Ghio AJ, Soukup JM, Dailey LA, Madden MC. Air pollutants disrupt iron homeostasis to impact oxidant generation, biological effects, and tissue injury. Free Radic Biol Med. 2020;151:38–55. [PubMed: 32092410]
3. Laughton MJ, Moroney MA, Hoult JR, Halliwell B. Effects of desferrioxamine on eicosanoid production in two intact cell systems. Biochem Pharmacol. 1989;38(1):189–193. [PubMed: 2491945]
4. Hileti D, Panayiotidis P, Hoffbrand AV. Iron chelators induce apoptosis in proliferating cells. Br J Haematol. 1995;89(1):181–187. [PubMed: 7833261]
5. Tanji K, Imaizumi T, Matsumiya T, et al. Desferrioxamine, an iron chelator, upregulates cyclooxygenase-2 expression and prostaglandin production in a human macrophage cell line. Biochim Biophys Acta. 2001;1530(2–3):227–235. [PubMed: 11239825]
6. Kim BS, Yoon KH, Oh HM, et al. Involvement of p38 MAP kinase during iron chelator-mediated apoptotic cell death. Cell Immunol. 2002;220(2):96–106. [PubMed: 12657244]
7. Lee SK, Jang HJ, Lee HJ, et al. p38 and ERK MAP kinase mediates iron chelator-induced apoptosis and -suppressed differentiation of immortalized and malignant human oral keratinocytes. Life Sci. 2006;79(15):1419–1427. [PubMed: 16697418]
8. Huang X, Dai J, Huang C, Zhang Q, Bhanot O, Pelle E. Deferoxamine synergistically enhances iron-mediated AP-1 activation: a showcase of the interplay between extracellular-signal-regulated kinase and tyrosine phosphatase. Free Radic Res. 2007;41(10):1135–1142. [PubMed: 17886035]
9. Markel TA, Crisostomo PR, Wang M, et al. Iron chelation acutely stimulates fetal human intestinal cell production of IL-6 and VEGF while decreasing HGF: the roles of p38, ERK, and JNK MAPK signaling. Am J Physiol Gastrointest Liver Physiol. 2007;292(4):G958–963. [PubMed: 17204543]

10. Liu Y, Cui Y, Shi M, Zhang Q, Wang Q, Chen X. Deferoxamine promotes MDA-MB-231 cell migration and invasion through increased ROS-dependent HIF-1alpha accumulation. Cell Physiol Biochem. 2014;33(4):1036–1046. [PubMed: 24732598]
11. Zhang W, Wu Y, Yan Q, et al. Deferoxamine enhances cell migration and invasion through promotion of HIF-1alpha expression and epithelial-mesenchymal transition in colorectal cancer. Oncol Rep. 2014;31(1):111–116. [PubMed: 24173124]
12. Ghio AJ, Soukup JM, Dailey LA. Air pollution particles and iron homeostasis. Biochim Biophys Acta. 2016.
13. Lovstad RA. The reaction of ferric- and ferrous salts with bleomycin. Int J Biochem. 1991;23(2):235–238. [PubMed: 1705524]
14. Ueda N, Guidet B, Shah SV. Gentamicin-induced mobilization of iron from renal cortical mitochondria. Am J Physiol. 1993;265(3 Pt 2):F435–439. [PubMed: 8214103]
15. Elias Z, Poirot O, Daniere MC, et al. Surface reactivity, cytotoxicity, and transforming potency of iron-covered compared to untreated refractory ceramic fibers. J Toxicol Environ Health A. 2002;65(23):2007–2027. [PubMed: 12490045]
16. Jacobson MC HH, Noone KJ, Charlson RJ. Organic atmospheric aerosols: review and state of the science. Reviews of Geophysics. 2000;38:267–294.
17. Dinar EMT, Rudich Y. The density of humic acids and humic like substances (HULIS) from fresh and aged wood burning and pollution aerosol particles. Atmos Chem Phys. 2006;6:5213–5224.
18. Graber ER, Rudich Y. Atmospheric HULIS: How humic-like are they? A comprehensive and critical review. Atmos Chem Phys. 2006;6:729–753.
19. Ghio AJ, Stonehuerner J, Pritchard RJ, Piantadosi CA, Quigley DR, Dreher KL, Costa DL Humic-like substances in air pollution particulates correlate with concentrations of transition metals and oxidant generation. Inhalation Toxicology. 1996;8:479–494.
20. Stedman RL, Chamberlain WJ, Miller RL. High molecular weight pigment in cigarette smoke. Chemistry & industry. 1966;37:1560–1562. [PubMed: 5915101]
21. Ghio AJ SJ, Quigley DR. Humic-like substances in cigarette condensate and lung tissue of smokers. Am J Physiol. 1994;266:L382–L388. [PubMed: 8179015]
22. Ghio A, Stonehuerner J, Pritchard RJ, Piantadosi CA, Quigley DR, Dreher KL, and Costa DL. Humic-like substances in air pollution particulates correlate with concentrations of transition metals and oxidant generation. Inhalation Toxicology. 1996;8:479–494.
23. Yang R, Van den Berg CM. Metal complexation by humic substances in seawater. Environ Sci Technol. 2009;43(19):7192–7197. [PubMed: 19848121]
24. Yamamoto M, Nishida A, Otsuka K, Komai T, Fukushima M. Evaluation of the binding of iron(II) to humic substances derived from a compost sample by a colorimetric method using ferrozine. Bioresour Technol. 2010;101(12):4456–4460. [PubMed: 20163958]
25. Town RM, Duval JF, Buffle J, van Leeuwen HP. Chemodynamics of metal complexation by natural soft colloids: Cu(II) binding by humic acid. The journal of physical chemistry A 2012;116(25):6489–6496. [PubMed: 22324832]
26. Erdogan S BA, Akba O, Hamamci C. . Interaction of metals with humic acid isolated from oxidized coal. . Polish J Environ Stud. 2007;16:671–675.
27. Bae S, Lim YH, Kashima S, et al. Non-Linear Concentration-Response Relationships between Ambient Ozone and Daily Mortality. PLoS One. 2015;10(6):e0129423. [PubMed: 26076447]
28. Crouse DL, Peters PA, Hystad P, et al. Ambient PM2.5, O(3), and NO(2) Exposures and Associations with Mortality over 16 Years of Follow-Up in the Canadian Census Health and Environment Cohort (CanCHEC). Environ Health Perspect. 2015;123(11):1180–1186. [PubMed: 26528712]
29. Di Q, Wang Y, Zanobetti A, et al. Air Pollution and Mortality in the Medicare Population. N Engl J Med. 2017;376(26):2513–2522. [PubMed: 28657878]
30. Yin P, Chen R, Wang L, et al. Ambient Ozone Pollution and Daily Mortality: A Study in 272 Chinese Cities. Environ Health Perspect. 2017;125(11):117006. [PubMed: 29212061]
31. Jakab GJ, Hemenway DR. Concomitant Exposure to Carbon-Black Particulates Enhances Ozone-Induced Lung Inflammation and Suppression of Alveolar Macrophage Phagocytosis. J Toxicol Env Health. 1994;41(2):221–31. [PubMed: 8301700]

32. Madden MC, Richards JH, Dailey LA, et al. Effect of ozone on diesel exhaust particle toxicity in rat lung. Toxicol Appl Pharmacol. 2000;168(2):140–8. [PubMed: 11032769]
33. Kafoury RM, Kelley J. Ozone enhances diesel exhaust particles (DEP)-induced interleukin-8 (IL-8) gene expression in human airway epithelial cells through activation of nuclear factors-kappaB (NF-kappaB) and IL-6 (NF-IL6). Int J Environ Res Public Health. 2005;2(3–4):403–10. [PubMed: 16819095]
34. Bosson J, Barath S, Pourazar J, et al. Diesel exhaust exposure enhances the ozone-induced airway inflammation in healthy humans. Eur Respir J. 2008;31(6): 1234–40. [PubMed: 18321939]
35. Stiegel MA, Pleil JD, Sobus JR, Madden MC. Inflammatory Cytokines and White Blood Cell Counts Response to Environmental Levels of Diesel Exhaust and Ozone Inhalation Exposures. PLoS One. 2016;11(4):e0152458 [PubMed: 27058360]
36. Risby TH, Sehnert SS. A model for the formation of airborne particulate matter based on the gas-phase adsorption on amorphous carbon blacks. Environ Health Perspect. 1988;77:131–140. [PubMed: 3383817]
37. Cataldo F Ozone reaction with carbon nanostructures 1: Reaction between solid C-60 and C-70 fullerenes and ozone. J Nanosci Nanotechno. 2007;7(4–5):1439–1445.
38. Cataldo F Ozone reaction with carbon nanostructures 2: The reaction of ozone with milled graphite and different carbon black grades. J Nanosci Nanotechno. 2007;7(4-5):1446–1454.
39. Chapleski RC, Morris JR, Troya D. A theoretical study of the ozonolysis of C60: primary ozonide formation, dissociation, and multiple ozone additions. Phys Chem Chem Phys. 2014;16(13):5977–5986. [PubMed: 24549406]
40. Tiwari AJ, Morris JR, Vejerano EP, Hochella MF, Marr LC. Oxidation of C-60 Aerosols by Atmospherically Relevant Levels of O-3. Environmental Science & Technology. 2014;48(5):2706–2714. [PubMed: 24517376]
41. Liu YC, Liggio J, Li SM, et al. Chemical and Toxicological Evolution of Carbon Nanotubes During Atmospherically Relevant Aging Processes. Environmental Science & Technology. 2015;49(5):2806–2814. [PubMed: 25607982]
42. Sutherland I, Sheng E, Bradley RH, Freakley PK. Effects of ozone oxidation on carbon black surfaces. J Mater Sci. 1996;31(21):5651–5655.
43. Ciobanu M LA, Asaftei S. Chemical and electrochemical studies of carbon black surface by treatment with ozone and nitrogen oxide. Materials Today – Proceedings 2016;3 (Supplement 2):S252–S257.
44. Smith DM, Chughtai AR. The Surface-Structure and Reactivity of Black Carbon. Colloid Surface A. 1995;105(1):47–77.
45. Chughtai AR, Miller NJ, Smith DM, Pitts JR. Carbonaceous particle hydration III. J Atmos Chem. 1999;34(2):259–279.
46. Chughtai AR, Jassim JA, Peterson JH, Stedman DH, Smith DM. Spectroscopic and Solubility Characteristics of Oxidized Soots. Aerosol Sci Tech. 1991;15(2):112–126.
47. Chughtai AR, Brooks ME, Smith DM. Hydration of black carbon. J Geophys Res-Atmos. 1996;101(D14):19505–19514.
48. Westerhoff P, Debroux J, Aiken G, Amy G. Ozone-induced changes in natural organic matter (NOM) structure. Ozone-Sci Eng. 1999;21(6):551–570.
49. Pollutants CoMaBEoE. Ozone and Other Photochemical Oxidants. Washington, D.C.: National Academy of Sciences; 1977.
50. Ghio AJ, Jaskot RH, Hatch GE. Lung injury after silica instillation is associated with an accumulation of iron in rats. Am J Physiol. 1994;267(6 Pt 1):L686–692. [PubMed: 7810673]
51. Koerten HK, Brederoo P, Ginsel LA, Daems WT. The endocytosis of asbestos by mouse peritoneal macrophages and its long-term effect on iron accumulation and labyrinth formation. Eur J Cell Biol. 1986;40(1):25–36. [PubMed: 3009191]
52. Ghio AJ, Stonehuerner J, Quigley DR. Humic-like substances in cigarette smoke condensate and lung tissue of smokers. Am J Physiol. 1994;266(4 Pt 1):L382–388. [PubMed: 8179015]
53. Ghio AJ, Soukup JM, Dailey LA, et al. Wood Smoke Particle Sequesters Cell Iron to Impact a Biological Effect. Chem Res Toxicol. 2015;28(11):2104–2111. [PubMed: 26462088]

54. Gonzalez DH, Soukup JM, Madden MC, et al. A fulvic acid-like substance participates in the pro-inflammatory effects of cigarette smoke and wood smoke particles. Chem Res Toxicol 2020;33(4):999–1009. [PubMed: 32191033]

55. Sporn TAaR VL Pneumoconioses, Mineral and Vegetable In: Tomashefski JFJ, Cagle PT, Farver CF, and Fraire AE, ed. Dail and Hammar's Pulmonary Pathology. Volume I. Nonneoplastic Lung Disease. 3rd ed.: Springer; 2008:933.

56. Gau RJ, Yang HL, Suen JL, Lu FJ. Induction of oxidative stress by humic acid through increasing intracellular iron: a possible mechanism leading to atherothrombotic vascular disorder in blackfoot disease. Biochem Biophys Res Commun. 2001;283(4):743–749. [PubMed: 11350046]

57. Hseu YC, Huang HW, Wang SY, et al. Humic acid induces apoptosis in human endothelial cells. Toxicol Appl Pharmacol. 2002;182(1):34–43. [PubMed: 12127261]

58. Cheng ML, Ho HY, Huang YW, Lu FJ, Chiu DT. Humic acid induces oxidative DNA damage, growth retardation, and apoptosis in human primary fibroblasts. Exp Biol Med (Maywood). 2003;228(4):413–423. [PubMed: 12671186]

59. Yang HL, Hseu YC, Hseu YT, Lu FJ, Lin E, Lai JS. Humic acid induces apoptosis in human premyelocytic leukemia HL-60 cells. Life Sci. 2004;75(15):1817–1831. [PubMed: 15302226]

60. Hseu YC, Lin E, Chen JY, et al. Humic acid induces G1 phase arrest and apoptosis in cultured vascular smooth muscle cells. Environ Toxicol. 2009;24(3):243–258. [PubMed: 18683188]

61. van Eijl S, Mortaz E, Ferreira AF, et al. Humic acid enhances cigarette smoke-induced lung emphysema in mice and IL-8 release of human monocytes. Pulm Pharmacol Ther. 2011;24(6):682–689. [PubMed: 21820074]

62. Hseu YC, Senthil Kumar KJ, Chen CS, et al. Humic acid in drinking well water induces inflammation through reactive oxygen species generation and activation of nuclear factor-kappaB/activator protein-1 signaling pathways: a possible role in atherosclerosis. Toxicol Appl Pharmacol. 2014;274(2):249–262. [PubMed: 24239652]

63. Shadie AM, Herbert C, Kumar RK. Ambient particulate matter induces an exacerbation of airway inflammation in experimental asthma: role of interleukin-33. Clin Exp Immunol. 2014;177(2):491–499. [PubMed: 24730559]

64. Chu H, Shang J, Jin M, et al. Comparison of lung damage in mice exposed to black carbon particles and 1,4-naphthoquinone coated black carbon particles. Sci Total Environ. 2017;580:572–581. [PubMed: 28034545]

65. Cervellati F, Woodby B, Benedusi M, et al. Evaluation of oxidative damage and Nrf2 activation by combined pollution exposure in lung epithelial cells. Environ Sci Pollut Res Int. 2020;27(25):31841–31853. [PubMed: 32504424]

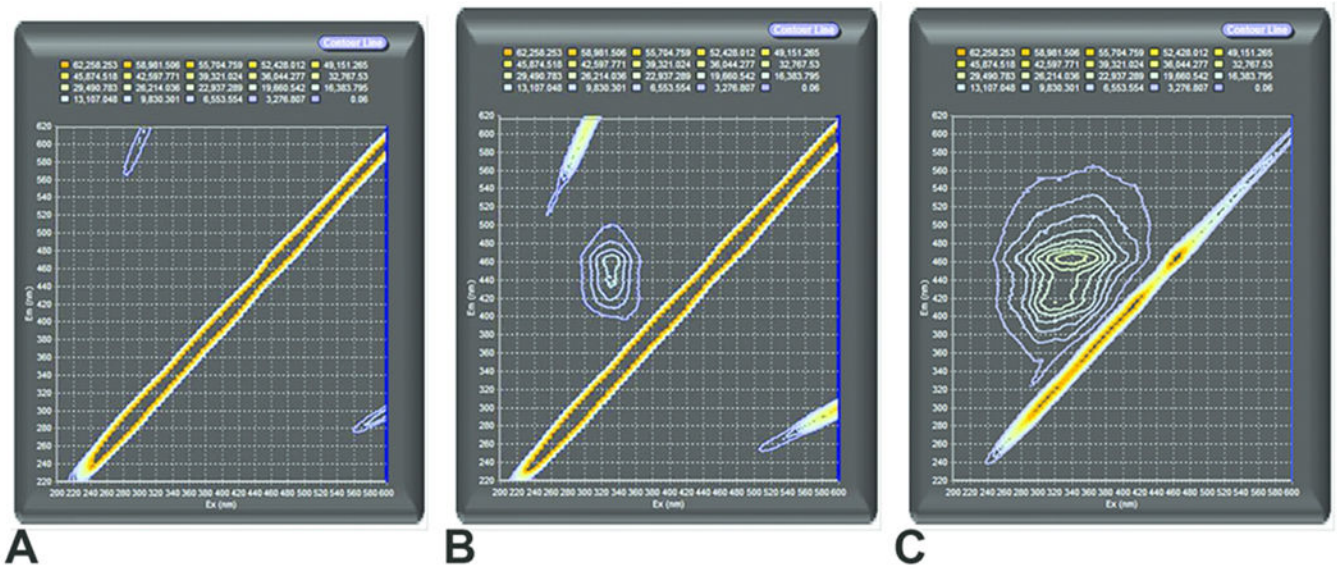

Figure 1.

Fluorescence excitation-emission matrix spectra of carbon black treated with air (CB-Air) (A), carbon black treated with ozone (CB-O_3) (B), and Suwanee River fulvic acid (SRFA) (C). The exposure of CB to high levels of ozone produced water-soluble, fluorescent organic material with similarities of fluorophores with SRFA. The diagonal line towards the right lower corner is an instrument artifact due to light scattering.

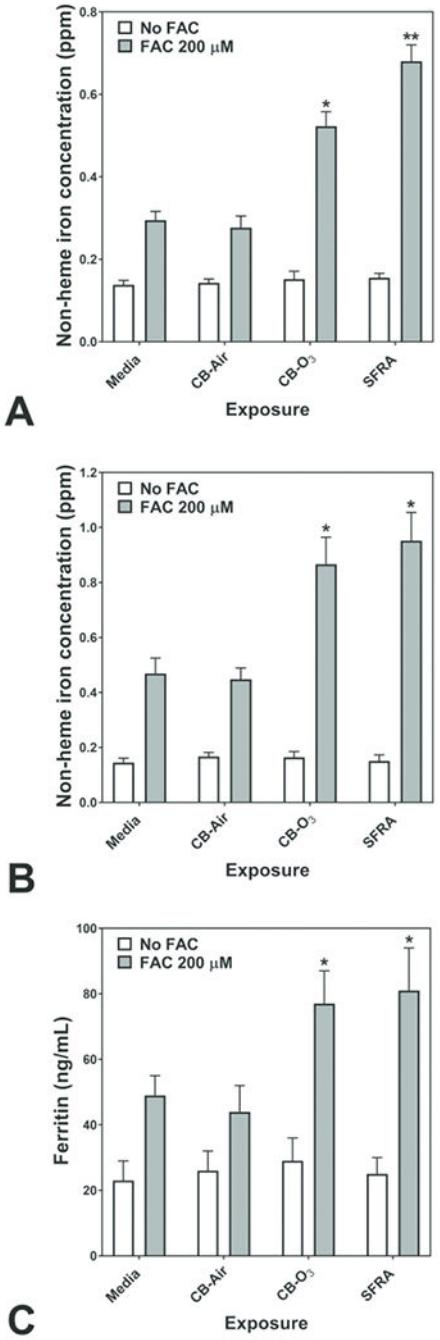

Figure 2.

Cell non-heme iron concentrations following 4 (A) and 24 (B) hr exposures of BEAS-2B cells to media, carbon black treated with air (CB-Air), carbon black treated with ozone (CB-O_3), and Suwanee River fulvic acid (SRFA). Incubations were without and with 200 μM FAC. Exposures to CB-Air, CB-O_3, and SRFA did not impact cell non-heme iron relative to media at either time point. Exposure to FAC increased cell non-heme iron but co-exposure with CB-O_3, was associated with significantly increased non-heme iron concentrations at both 4 (A) and 24 (B) hr. Exposures of BEAS-2B cells to FAC increased cell ferritin levels

after 24 hr relative to media alone (C). However, co-exposure of CB-O_3, and SRFA with FAC was associated with significantly elevated cell ferritin concentrations (C). Two-way ANOVA indicated that both addition of FAC and exposure group significantly impacted cell non-heme iron. Among the cell exposures with addition of FAC, one-way ANOVA demonstrated: * significant increase relative to exposure of BEAS-2B cells to media only and ** significant increase relative to all other exposures.

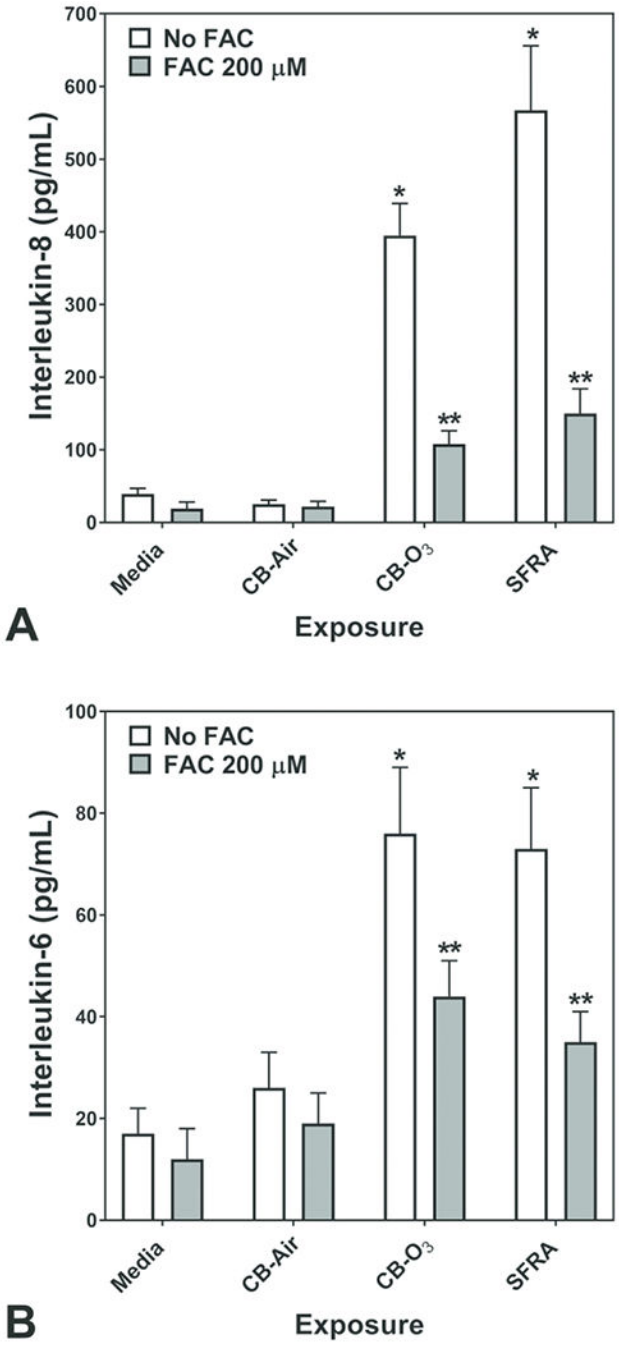

Figure 3.

Release of IL-8 and IL-6 after 24 hr exposure of BEAS-2B cells to media, carbon black treated with air (CB-Air), carbon black treated with ozone (CB-O_3), and Suwanee River fulvic acid (SRFA). Exposure to CB-O_3, and SRFA significantly increased the release of IL-8 and IL-6. FAC treatment significantly diminished this response. One-way ANOVA demonstrated: * significant increase relative to all other exposures and ** significant increase relative to media exposure.

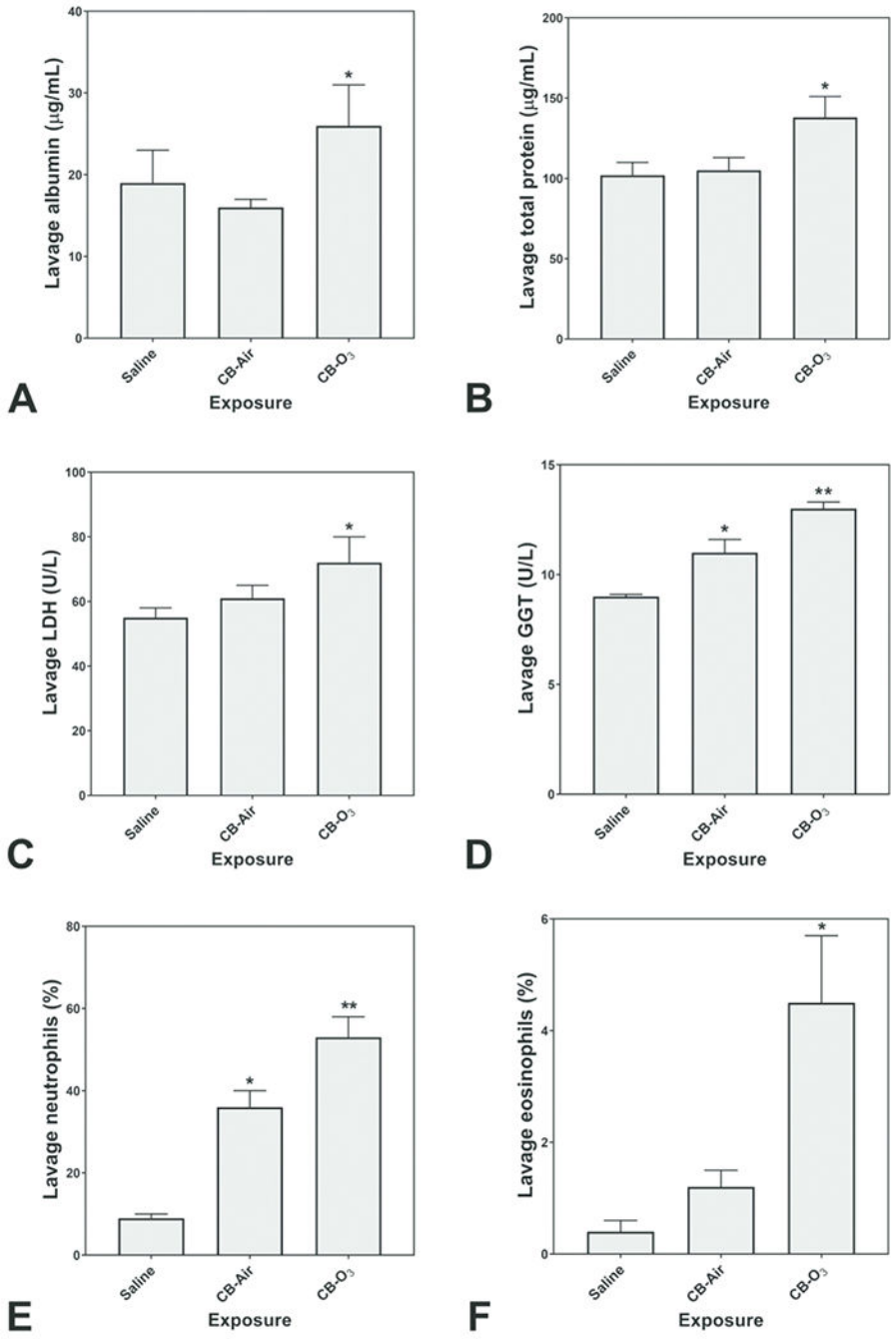

Figure 4.

Lavage indices of injury and inflammation following animal exposures to normal saline, carbon black treated with air (CB-Air), and carbon black treated with ozone (CB-O_3). There is evidence of both injury and inflammation following both CB-Air and CB-O_3 but both are significantly greater following CB-O_3. One-way ANOVA demonstrated: * significant increase relative to exposure of animals to saline only and ** significant increase relative to all other exposures.

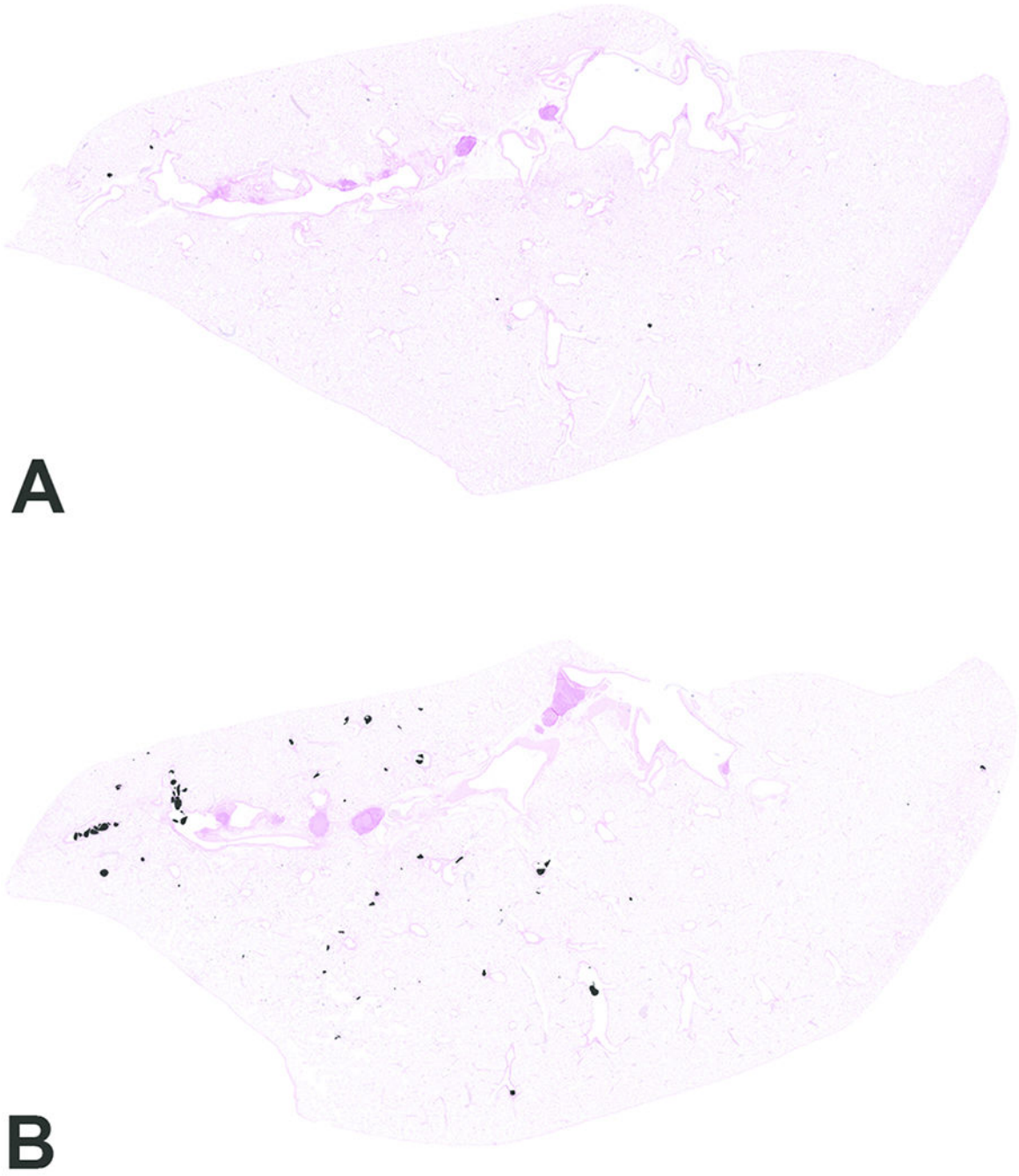

Figure 5.
Scanned images of lung pathology following animal exposures to carbon black treated with air (CB-Air; A) or ozone (CB-O_3; B). There are increased numbers of particles and the particles are larger in size in CB-O_3 (B) animals compared to CB-Air (A) animals. Tissues were stained with Prussian blue to better illustrate the particles. Original scans at 1x.

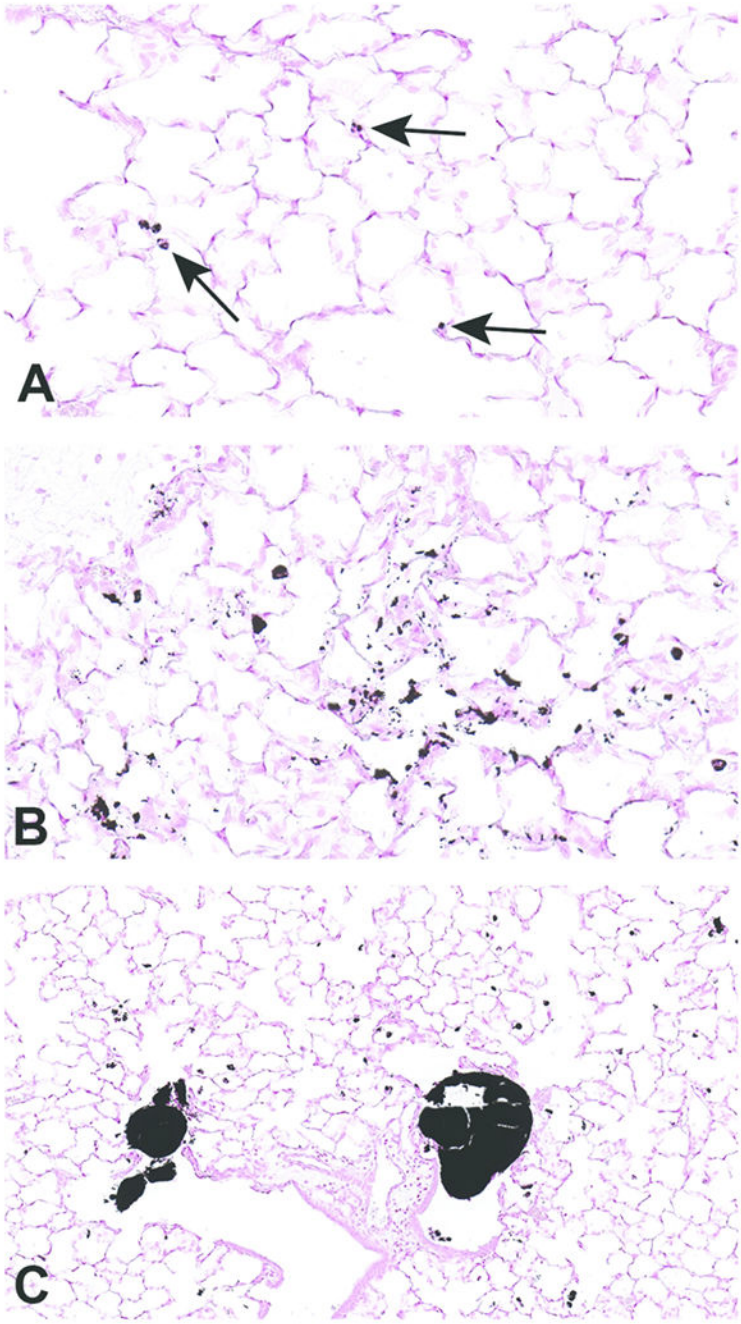

Figure 6.

Scanned images of lung pathology following exposures to carbon black treated with air (CB-Air; A) or ozone (CB-O_3; B). Figures 6A and 6B are higher magnification images (original scans at 40x) of figures 5A and 5B, respectively. Particles in A are indicated with arrows. There was an increased number and size of particles in CB-O_3 (B) lungs compared to CB-Air (A) lungs. Figure C illustrates the scattered larger particles in CB-O_3 lungs (original scan at 20x). The larger aggregates were predominately in the terminal bronchi and alveolar ducts. Tissues were stained with Prussian blue to better illustrate the particles.

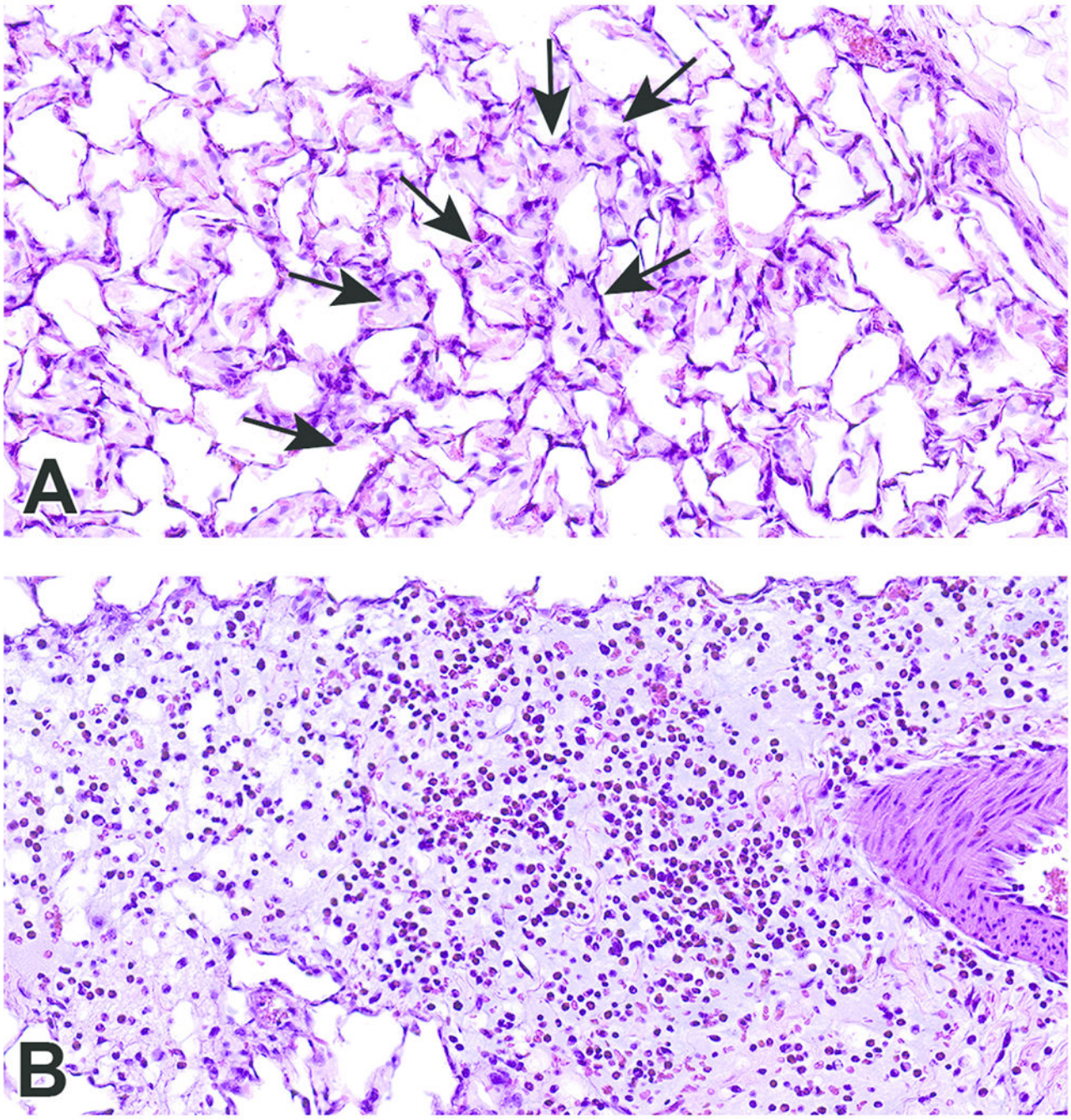

Figure 7.

Scanned images show examples of macrophage infiltrates within alveoli (A; arrows) and perivascular and peribronchiolar interstitial inflammation (B) in animals exposed to CB-O_3. Edema is present in the perivascular and peribronchiolar regions of inflammation. Macrophages and granulocytic infiltrates were increased in the CB-O_3 group compared to the CB-air group. Original scans at 40x; stain is hematoxylin and eosin.

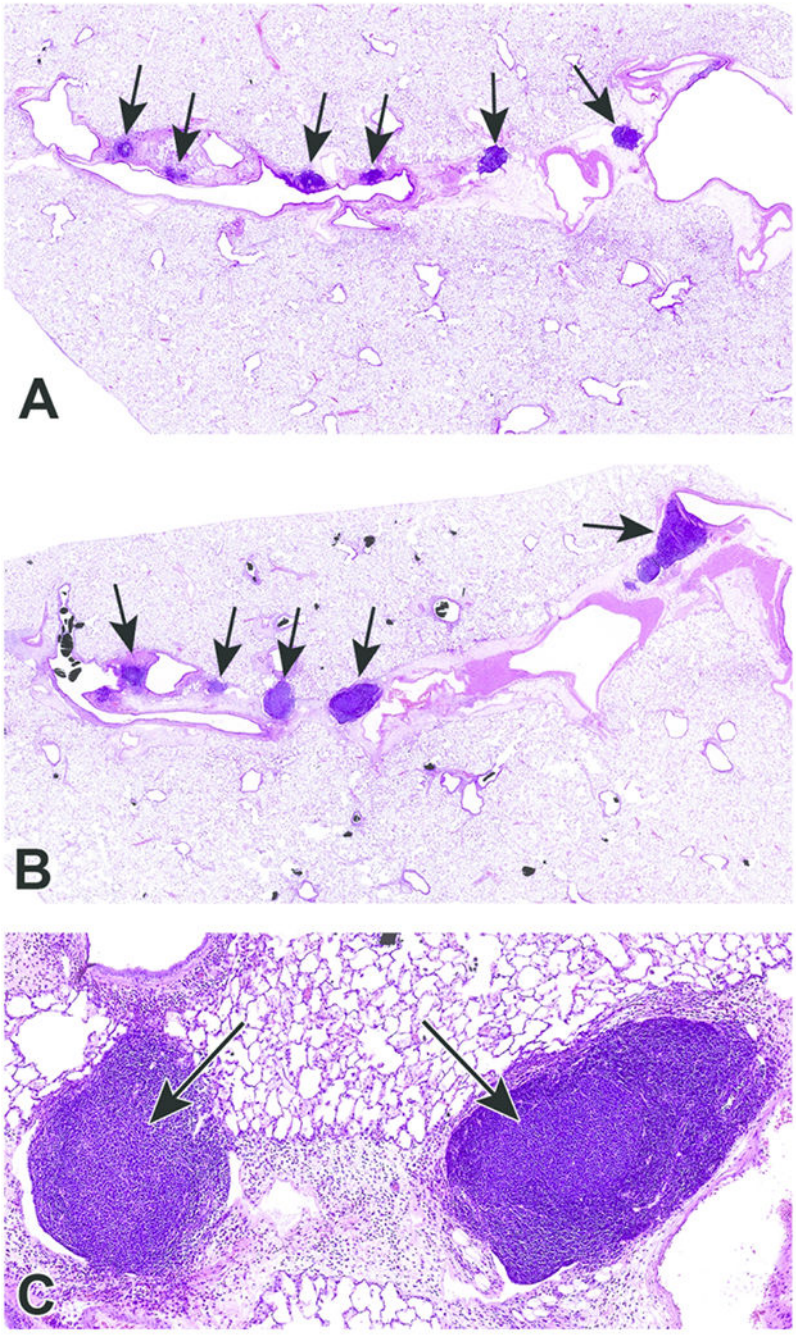

Figure 8.

Photomicrographs of bronchioalveolar lymphoid aggregates (BALT) in animals exposed to CB-Air (A) and CB-O_3 (B). BALT was increased in the CB-O_3 (B; arrows) group relative to the CB-Air group (A; arrows) and CB-O_3 lungs typically had prominent germinal centers (C; arrows). A and B original scans at 2x while C original scan at 14x; stain is hematoxylin and eosin.

Table 1

Summary of Common Infrared Absorption Peaks among Samples

Bond	Functional group	CB-O_3 [a] (λ in nm)	SRFA [b] (λ in nm)
O-H	Alcohols, phenols, carboxylic acids	3304-3374	3382
C-H	Aromatic	2917	2942
C=O	Ketones, carboxylic acids, aldehydes	1700-1723	1713
C=C and C=O	Aromatic	1634-1639	1624
C=H	Alkane	None	1387
C-O	Ether, acids	1189-1187	1202

[a] CB-O3 = carbon black treated with ozone

[b] SRFA = Suwanee River fulvic acid

Toxicol Pathol. Author manuscript; available in PMC 2021 January 15.